

**Advances in Bioscience and Bioengineering**

2017; 5(2): 22-31

<http://www.sciencepublishinggroup.com/j/abb>

doi: 10.11648/j.abb.20170502.11

ISSN: 2330-4154 (Print); ISSN: 2330-4162 (Online)

**SciencePG**

Science Publishing Group

# LC-MS and NMR Based Structural Characterization and Isotopic Abundance Ratio Analysis of Magnesium Gluconate Treated with the Consciousness Energy Healing

Mahendra Kumar Trivedi<sup>1</sup>, Alice Branton<sup>1</sup>, Dahryn Trivedi<sup>1</sup>, Gopal Nayak<sup>1</sup>, William Dean Plikerd<sup>1</sup>, Peter L. Surguy<sup>1</sup>, Robert John Kock<sup>1</sup>, Rolando Baptista Piedad<sup>1</sup>, Russell Phillip Callas<sup>1</sup>, Sakina A. Ansari<sup>1</sup>, Sandra Lee Barrett<sup>1</sup>, Sara Friedman<sup>1</sup>, Steven Lee Christie<sup>1</sup>, Su-Mei Chen Liu<sup>1</sup>, Susan Elizabeth Starling<sup>1</sup>, Susan Jones<sup>1</sup>, Susan Mardis Allen<sup>1</sup>, Susanne Kathrin Wasmus<sup>1</sup>, Terry Ann Benczik<sup>1</sup>, Thomas Charles Slade<sup>1</sup>, Thomas Orban<sup>1</sup>, Victoria L. Vannes<sup>1</sup>, Victoria Margot Schlosser<sup>1</sup>, Yusif Sarkis Yamin Albino<sup>1</sup>, Parthasarathi Panda<sup>2</sup>, Kalyan Kumar Sethi<sup>2</sup>, Snehasis Jana<sup>2,\*</sup>

<sup>1</sup>Trivedi Global, Inc., Henderson, Nevada, USA<sup>2</sup>Trivedi Science Research Laboratory Pvt. Ltd., Bhopal, Madhya Pradesh, India**Email address:**[publication@trivedieffect.com](mailto:publication@trivedieffect.com) (S. Jana)

\*Corresponding author

**To cite this article:**

Mahendra Kumar Trivedi, Alice Branton, Dahryn Trivedi, Gopal Nayak, William Dean Plikerd, Peter L. Surguy, Robert John Kock, Rolando Baptista Piedad, Russell Phillip Callas, Sakina A. Ansari, Sandra Lee Barrett, Sara Friedman, Steven Lee Christie, Su-Mei Chen Liu, Susan Elizabeth Starling, Susan Jones, Susan Mardis Allen, Susanne Kathrin Wasmus, Terry Ann Benczik, Thomas Charles Slade, Thomas Orban, Victoria L. Vannes, Victoria Margot Schlosser, Yusif Sarkis Yamin Albino, Parthasarathi Panda, Kalyan Kumar Sethi, Snehasis Jana. LC-MS and NMR Based Structural Characterization and Isotopic Abundance Ratio Analysis of Magnesium Gluconate Treated with the Consciousness Energy Healing. *Advances in Bioscience and Bioengineering*. Vol. 5, No. 2, 2017, pp. 22-31. doi: 10.11648/j.abb.20170502.11

**Received:** February 24, 2017; **Accepted:** March 8, 2017; **Published:** April 1, 2017

**Abstract:** Magnesium gluconate is widely used pharmaceutical/nutraceutical compound for the prevention and treatment of magnesium deficiency diseases. The present study was designed to explore the effect of The Trivedi Effect<sup>®</sup> - Energy of Consciousness Healing Treatment (Biofield Energy Healing Treatment) on magnesium gluconate for the change in the structural properties and isotopic abundance ratio ( $P_{M+1}/P_M$  and  $P_{M+2}/P_M$ ) using LC-MS and NMR spectroscopy. Magnesium gluconate was divided into two parts – one part was control, and another part was treated with The Trivedi Effect<sup>®</sup> - Energy of Consciousness Healing Treatment remotely by twenty renowned Biofield Energy Healers and defined as The Trivedi Effect<sup>®</sup> treated sample. The LC-MS analysis of both the control and Biofield Energy Treated samples indicated the presence of mass of the protonated magnesium gluconate at  $m/z$  415 at the retention time of 1.52 min and fragmentation pattern of both samples were almost identical. The relative peak intensities of the fragment ions were significantly altered in the treated sample compared to the control sample. The proton and carbon signals for CH, CH<sub>2</sub> and CO groups in the proton and carbon NMR spectra of the control and treated samples were found same. The percentage change in the isotopic abundance ratio of  $P_{M+1}/P_M$  ( $^2\text{H}/^1\text{H}$  or  $^{13}\text{C}/^{12}\text{C}$  or  $^{17}\text{O}/^{16}\text{O}$  or  $^{25}\text{Mg}/^{24}\text{Mg}$ ) was significantly decreased in the treated sample by 48.87% compared to the control sample. Subsequently, the isotopic abundance ratio of  $P_{M+2}/P_M$  ( $^{18}\text{O}/^{16}\text{O}$  or  $^{26}\text{Mg}/^{24}\text{Mg}$ ) in the treated sample was significantly increased by 29.18% compared with the control sample. In summary,  $^{13}\text{C}$ ,  $^2\text{H}$ ,  $^{17}\text{O}$ , and  $^{25}\text{Mg}$  contributions from  $(\text{C}_{12}\text{H}_{23}\text{MgO}_{14})^+$  to  $m/z$  416;  $^{18}\text{O}$  and  $^{26}\text{Mg}$  contributions from  $(\text{C}_{12}\text{H}_{23}\text{MgO}_{14})^+$  to  $m/z$  417 in the treated sample were significantly altered compared with the control sample. Thus, The Trivedi Effect<sup>®</sup> Treated magnesium gluconate might be helpful to design the novel potent enzyme inhibitors using its kinetic isotope effects. Consequently, The Trivedi Effect<sup>®</sup> Treated magnesium gluconate would be valuable for designing better pharmaceutical and/or nutraceutical formulations through its altered physicochemical and thermal properties, which might be providing better therapeutic response against various diseases such as diabetes mellitus, allergy, aging, inflammatory diseases, immunological disorders, and other chronic infections.

**Keywords:** Magnesium Gluconate, The Trivedi Effect<sup>®</sup>, Consciousness Energy Healing Treatment, Biofield Energy Healing Treatment, Isotope Effects, Biofield Energy Healers, LC-MS, Isotopic Abundance

## 1. Introduction

Magnesium gluconate is an organometallic salt of magnesium with gluconic acid for the source of magnesium ion [1]. Magnesium is an essential mineral in our body, as it acts as cofactor for more than 300 enzymes, synthesis of DNA, RNA, reproduction, and protein as well as an important coherent controller of glycolysis and the Krebs cycle [2, 3]. Hypomagnesemia may cause several diseases and disorders [4-7]. Magnesium gluconate is found to be the most physiologically acceptable salt, antioxidant and exhibited the highest level of bioavailability of magnesium among the available magnesium salts [8-10]. Therefore, magnesium gluconate is used for the prevention and treatment of diabetes mellitus, allergies, cardiovascular diseases, septic shock, inflammatory diseases, immunological disorders, arrhythmias, acute myocardial infarction, gestational hypertension, preeclampsia, eclampsia, Alzheimer's disease, cancer, and oxidative stress induced ischemia/reperfusion injury [4-7, 9-11]. It can be used as neuroprotective [12], an oral tocolytic agent [13], and also in a skin-tightening cosmetic composition [14]. In this point of view, a novel proprietary herbomineral formulation was designed as a nutraceutical supplement, and can be used for the prevention and treatment of various human disorders. Magnesium gluconate is one of the components in this novel proprietary herbomineral formulation as the source of magnesium.

Since ancient times, many different cultures, religions and systems of belief have recognized a living force that preserves and inhabits every living organism. This force is the source of 'life' and has been called various names, such as prana by the Hindus, *qi* or *chi* by the Chinese, and *ki* by the Japanese. This is believed to co-relate with the soul, spirit and mind. This hypothetical vital force has been scientifically evaluated and is now considered the Bioenergetics Field. The Biofield Energy is a dynamic electromagnetic field surrounding the human body, resulting from the continuous emission of low-level light, heat, and acoustical energy from the body. Biofield Energy is infinite, para-dimensional and can freely flow between the human and environment [15]. F. Sances *et al.* reported that Biofield Energy can be transmitted into any living organism (s) or nonliving object (s) around the globe with scientifically measurable effect through the intentional mental energies by specific energy healers [16]. The object or recipient always receives the energy from the ionosphere of the earth, the "universal energy field" and responds in a useful way. This process is known as The Trivedi Effect<sup>®</sup> - Energy of Consciousness Healing Treatment [17, 18]. Biofield (Putative Energy Field) based

Energy Therapies are used worldwide to promote health and healing. The National Center of Complementary and Integrative Health (NCCIH) has recognized and accepted Biofield Energy Healing as a Complementary and Alternative Medicine (CAM) health care approach in addition to other therapies, medicines and practices such as natural products, deep breathing, yoga, Tai Chi, Qi Gong, chiropractic/osteopathic manipulation, meditation, massage, special diets, homeopathy, progressive relaxation, guided imagery, acupressure, acupuncture, relaxation techniques, hypnotherapy, healing touch, movement therapy, pilates, rolfing structural integration, mindfulness, Ayurvedic medicine, traditional Chinese herbs and medicines, naturopathy, essential oils, aromatherapy, Reiki, cranial sacral therapy and applied prayer (as is common in all religions, like Christianity, Hinduism, Buddhism and Judaism) [19]. Biofield Energy Treatment (The Trivedi Effect<sup>®</sup>) has been drawn attention more in the recent times for its scientifically measurable capability to transform the characteristic properties of a wide varieties living and non-living substances such as plants [20, 21], animals [22], microbes [23, 24], cancer cells [25], medium [26, 27], materials [28, 29], pharmaceuticals [30, 31], nutraceuticals [32, 33], organic compounds [34, 35]. The scientific study indicated that Biofield Energy Healing Treatment (The Trivedi Effect<sup>®</sup>) might be an alternate method for increasing or decreasing the natural isotopic abundance ratio of the substances [36-39]. The stable isotope ratio analysis has the broad application in several scientific fields for understanding the isotope effects resulting from the difference of the isotopic composition of the molecule [40, 41]. Conventional mass spectrometry (MS) techniques such as liquid chromatography-mass spectrometry (LC-MS), gas chromatography-mass spectrometry (GC-MS) are extensively used for isotope ratio analysis with sufficient precision [42]. Hence, LC-MS and NMR (Nuclear Magnetic Resonance) methods were used in this research work to examine the effect of Biofield Energy Healing Treatment on structural properties of the Biofield Energy Treated and untreated magnesium gluconate. Consequently, the authors sought to explore the impact of The Trivedi Effect<sup>®</sup> - Energy of Consciousness Healing Treatment on the isotopic abundance ratios of  $P_{M+1}/P_M$  and  $P_{M+2}/P_M$  in magnesium gluconate through LC-MS based isotopic abundance ratio analysis in both the Biofield Energy Treated and untreated samples.

## 2. Materials and Methods

### 2.1. Chemicals and Reagents

Magnesium gluconate hydrate was purchased from Tokyo Chemical Industry Co., Ltd. (TCI), Japan. All other

chemicals used in the experiment were of analytical grade available in India.

## 2.2. Energy of Consciousness Healing Treatment Strategies

Magnesium gluconate was one of the components of the new proprietary herbomineral formulation, which was developed by our research team and was used *per se* as the test compound for the current study. The test compound was divided into two parts, one part of the test compound did not receive any sort of treatment and was defined as the untreated or control magnesium gluconate sample. The second part of the test compound was subjected to The Trivedi Effect® - Energy of Consciousness Healing Treatment (Biofield Energy Healing Treatment) by a group of twenty renowned Biofield Energy Healers remotely and was denoted as the Biofield Energy Treated or The Trivedi Effect® Treated sample. Fifteen Biofield Energy Healers were remotely located in the U.S.A., two in Canada, one in the UK, one in Australia, and one in Germany. The test compound was located in the research laboratory of GVK Biosciences Pvt. Ltd., Hyderabad, India. The Trivedi Effect® - Energy of Consciousness Healing Treatment (Biofield Energy Healing Treatment) was provided for 5 minutes through the Healer's Unique Energy Transmission process remotely to the test compound, which was kept under laboratory conditions. None of the Biofield Energy Healers in this study visited the laboratory in person, nor had any contact with the compounds. Similarly, the control compound was subjected to "sham" healer for 5 minutes, under the same laboratory conditions. The sham healer did not have any knowledge about the Biofield Energy Treatment. After that, The Trivedi Effect® Treated and untreated samples were kept in similar sealed conditions and characterized thoroughly by LC-MS and NMR spectroscopy.

## 2.3. Liquid Chromatography Mass Spectrometry (LC-MS) Analysis

Liquid chromatography was performed using The Waters® ACQUITY UPLC, Milford, MA, USA equipped with a binary pump (The Waters® BSM HPLC pump), autosampler, column heater and a photo-diode array (PDA) detector. The column used for the study was a reversed phase Acquity BEH shield RP C18 (150 X 3.0 mm, 2.5 µm). The column temperature was kept constant at 40°C. The mobile phase was 2mM ammonium acetate in water as mobile phase A and acetonitrile as mobile phase B. Chromatographic separation was achieved with following gradient program: 0 min – 5%B; 1 min – 5%B; 15 min - 97%B; 20 min – 97%B; 21 min – 5%B; 25 min – 5%B. The flow rate was at a constant flow rate of 0.4

mL/min. The control and Biofield Energy Treated samples were dissolved in a mixture of water and methanol (60:40 v/v) to prepare a 1 mg/mL stock solution. An aliquot of 2 µL of the stock solution was used for analysis by LC-ESI-MS and the total run time was 25 min.

Mass spectrometric analysis was accompanied on a Triple Quad (Waters Quattro Premier XE, USA) mass spectrometer equipped with an electrospray ionization (ESI) source with the following parameters: electrospray capillary voltage 3.5 kV; source temperature 100°C; desolvation temperature 350°C; cone voltage 30 V; desolvation gas flow 1000 L/h and cone gas flow 60 L/h. Nitrogen was used in the electrospray ionization source. The multiplier voltage was set at 650 V. LC-MS was taken in positive ionization mode and with the full scan ( $m/z$  50-1400). The total ion chromatogram, % peak area and mass spectrum of the individual peak (appeared in LC) were recorded.

## 2.4. Isotopic Abundance Ratio Analysis

The relative intensity of the peak in the mass spectra is directly proportional to the relative isotopic abundance of the molecule and the isotopic abundance ratio analysis was followed by the scientific literature reported [36-39] method described as below:

$P_M$  stands for the relative peak intensity of the parent molecular ion  $[M^+]$  expressed in percentage. In other way, it indicates the probability to  $A$  elements having only one natural isotope in appreciable abundance (for e.g.  $^{12}\text{C}$ ,  $^1\text{H}$ ,  $^{16}\text{O}$ ,  $^{24}\text{Mg}$ , etc.) contributions to the mass of the parent molecular ion  $[M^+]$ .

$P_{M+1}$  represents the relative peak intensity of the isotopic molecular ion  $[(M+1)^+]$  expressed in percentage

$$= (\text{no. of } ^{13}\text{C} \times 1.1\%) + (\text{no. of } ^{15}\text{N} \times 0.40\%) + (\text{no. of } ^2\text{H} \times 0.015\%) + (\text{no. of } ^{17}\text{O} \times 0.04\%) + (\text{no. of } ^{25}\text{Mg} \times 12.66\%)$$

i.e. the probability to  $A + 1$  elements having an isotope that has one mass unit heavier than the most abundant isotope (for e.g.  $^{13}\text{C}$ ,  $^2\text{H}$ ,  $^{17}\text{O}$ ,  $^{25}\text{Mg}$ , etc.) contributions to the mass of the isotopic molecular ion  $[(M+1)^+]$ .

$P_{M+2}$  represents the relative peak intensity of the isotopic molecular ion  $[(M+2)^+]$  expressed in the percentage

$$= (\text{no. of } ^{18}\text{O} \times 0.20\%) + (\text{no. of } ^{26}\text{Mg} \times 13.94\%)$$

i.e. the probability to have  $A + 2$  elements having an isotope that has two mass unit heavier than the most abundant isotope (for e.g.  $^{18}\text{O}$ ,  $^{26}\text{Mg}$ , etc.) contributions to the mass of isotopic molecular ion  $[(M+2)^+]$ .

**Table 1.** The isotopic composition (i.e. the natural isotopic abundance) of the elements.

Element	Symbol	Mass	% Natural Abundance	A+1 Factor	A+2 Factor
Hydrogen	<sup>1</sup> H	1	99.9885	0.015n <sub>H</sub>	
	<sup>2</sup> H	2	0.0115		
Carbon	<sup>12</sup> C	12	98.892	1.1 n <sub>C</sub>	
	<sup>13</sup> C	13	1.108		
Oxygen	<sup>16</sup> O	16	99.762	0.04 n <sub>O</sub>	0.20 n <sub>O</sub>
	<sup>17</sup> O	17	0.038		
	<sup>18</sup> O	18	0.200		
Magnesium	<sup>24</sup> Mg	24	78.99	12.66 n <sub>Mg</sub>	13.94 n <sub>Mg</sub>
	<sup>25</sup> Mg	25	10.00		
	<sup>26</sup> Mg	26	11.01		

A represents element, n represents the number of the element (i.e. C, H, O, Mg, etc.)

The value of the natural isotopic abundance of the elements used here for the theoretical calculation are achieved from the scientific literature and are presented in the Table 1 [43, 44].

Isotopic abundance ratio for A + 1 elements =  $P_{M+1}/P_M$

Similarly, isotopic abundance ratio for A + 2 elements =  $P_{M+2}/P_M$

Percentage (%) change in isotopic abundance ratio =

$$[(IAR_{\text{Treated}} - IAR_{\text{Control}}) / IAR_{\text{Control}}] \times 100 \quad (1)$$

Where,  $IAR_{\text{Treated}}$  = isotopic abundance ratio in the treated sample and  $IAR_{\text{Control}}$  = isotopic abundance ratio in the control sample.

## 2.5. Nuclear Magnetic Resonance (NMR) Analysis

<sup>1</sup>H NMR spectra were recorded in a 400 MHz VARIAN FT-NMR spectrometer at room temperature. Data refer to solutions in D<sub>2</sub>O with the residual solvent protons as internal

references. <sup>1</sup>H NMR multiplicities were designated as singlet (s), doublet (d), triplet (t), multiplet (m), and broad (br). <sup>13</sup>C NMR spectra were measured at 100 MHz on a VARIAN FT-NMR spectrometer at room temperature. Chemical shifts (δ) were in parts per million (ppm) relative to the solvent's residual proton chemical shift (D<sub>2</sub>O, δ = 4.65 ppm) and solvent's residual carbon chemical shift (D<sub>2</sub>O, δ = 0 ppm).

## 3. Results and Discussion

### 3.1. Liquid Chromatography-Mass Spectrometry (LC-MS) Analysis

A sharp and narrow peak was found in both the liquid chromatograms of the control and treated magnesium gluconate (Figure 1) at the retention time (R<sub>t</sub>) of 1.52 min indicating that the polarity/affinity of the treated sample remained identical compared to the control sample. The ESI-MS spectra of both the control and treated magnesium gluconate at R<sub>t</sub> of 1.52 min (Figure 2) showed the presence of the mass of magnesium gluconate at m/z 415 [M + H]<sup>+</sup> (calcd for C<sub>12</sub>H<sub>23</sub>MgO<sub>14</sub><sup>+</sup>, 415).

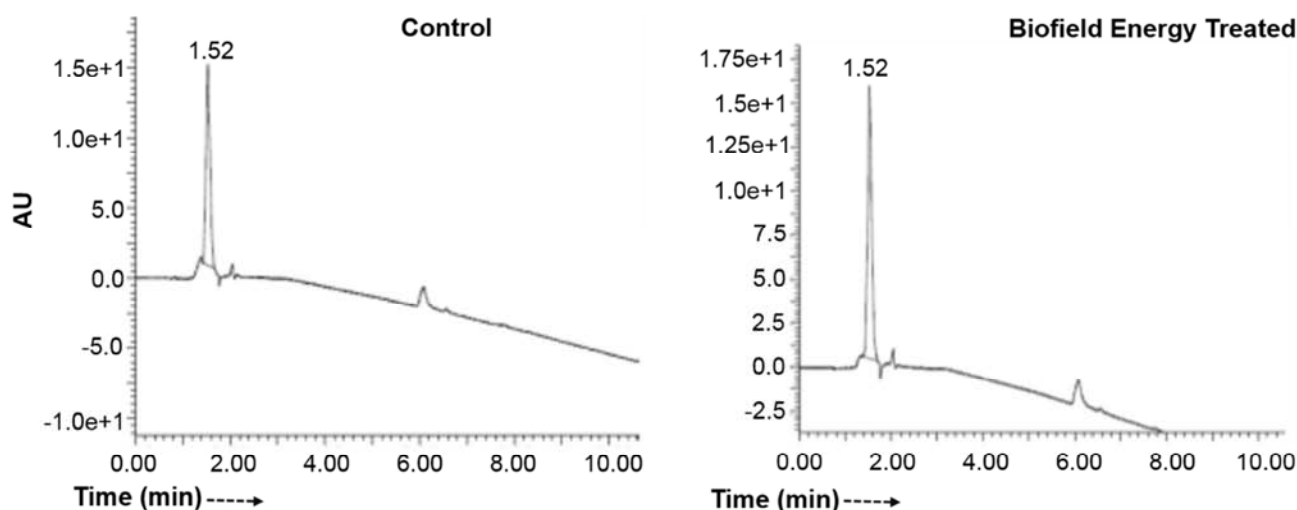


**Figure 1.** Liquid chromatograms of the control and Biofield Energy Treated magnesium gluconate.

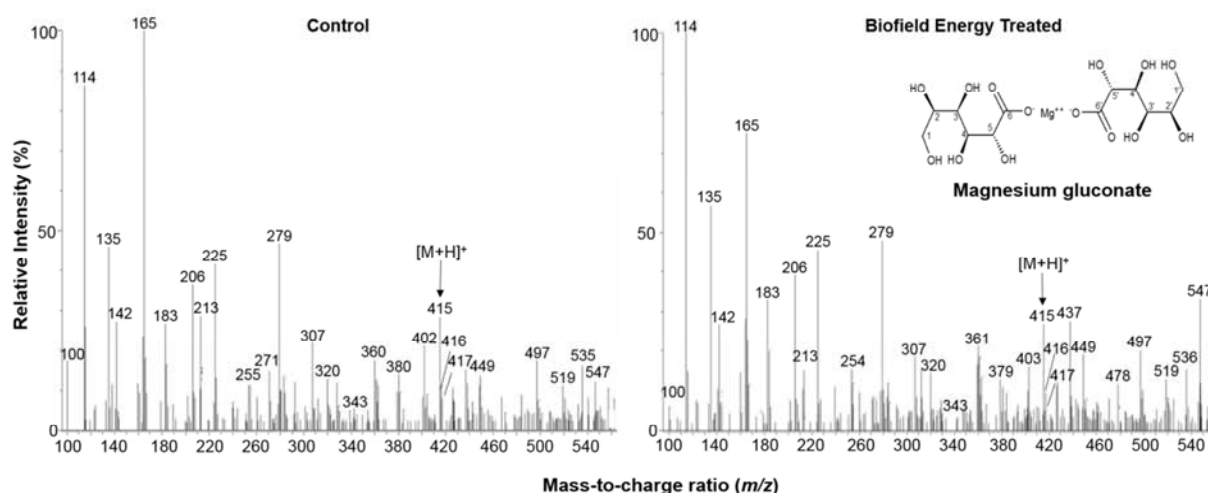


Figure 2. The ESI-MS spectra of the control and Biofield Energy Treated magnesium gluconate.

The notable fragment ion peaks in the lower  $m/z$  region of the molecular ion peak at  $m/z$  415 were observed in the control sample at  $m/z$  402, 380, 360, 343, 320, 307, 279, 271, 255, 225, 213, 206, 183, 165, 142, 135, 114, and 100 which correspond to the following molecular formula  $C_{12}H_{26}MgO_{13}^{4+}$ ,  $C_{12}H_{20}MgO_{12}^{+}$ ,  $C_{12}H_{16}MgO_{11}^{2+}$ ,  $C_{12}H_{15}MgO_{10}^{+}$ ,  $C_{10}H_{16}MgO_{10}^{+}$ ,  $C_9H_{15}MgO_{10}^{+}$ ,  $C_9H_3MgO_9^{2+}$ ,  $C_9H_{11}MgO_8^{+}$ ,  $C_9H_{11}MgO_7^{+}$ ,  $C_8H_9MgO_6^{+}$ ,  $C_7H_9MgO_6^{+}$ ,  $C_8H_6MgO_5^{2+}$ ,  $C_6H_7MgO_5^{+}$ ,  $C_5H_9O_6^{+}$ ,  $C_5H_2O_5^{2+}$ ,  $C_5H_{11}O_4^{+}$ ,

$C_5H_6O_3^{2+}$ , and  $C_4H_4O_3^{2+}$ , respectively as shown in the Figure 3. Consequently, the treated sample exhibited the fragment ion peaks at  $m/z$  403, 379, 361, 343, 320, 307, 279, 254, 225, 213, 206, 183, 165, 142, 135, 114, and 100 corresponding to the molecular formula  $C_{12}H_{27}MgO_{13}^{5+}$ ,  $C_{12}H_{19}MgO_{12}^{+}$ ,  $C_{12}H_{17}MgO_{11}^{+}$ ,  $C_{12}H_{15}MgO_{10}^{+}$ ,  $C_{10}H_{16}MgO_{10}^{+}$ ,  $C_9H_{15}MgO_{10}^{+}$ ,  $C_9H_3MgO_9^{2+}$ ,  $C_9H_{10}MgO_7^{2+}$ ,  $C_8H_9MgO_6^{+}$ ,  $C_7H_9MgO_6^{+}$ ,  $C_8H_6MgO_5^{2+}$ ,  $C_6H_7MgO_5^{+}$ ,  $C_5H_9O_6^{+}$ ,  $C_5H_2O_5^{2+}$ ,  $C_5H_{11}O_4^{+}$ ,  $C_5H_6O_3^{2+}$ , and  $C_4H_4O_3^{2+}$ , respectively (Figure 3).

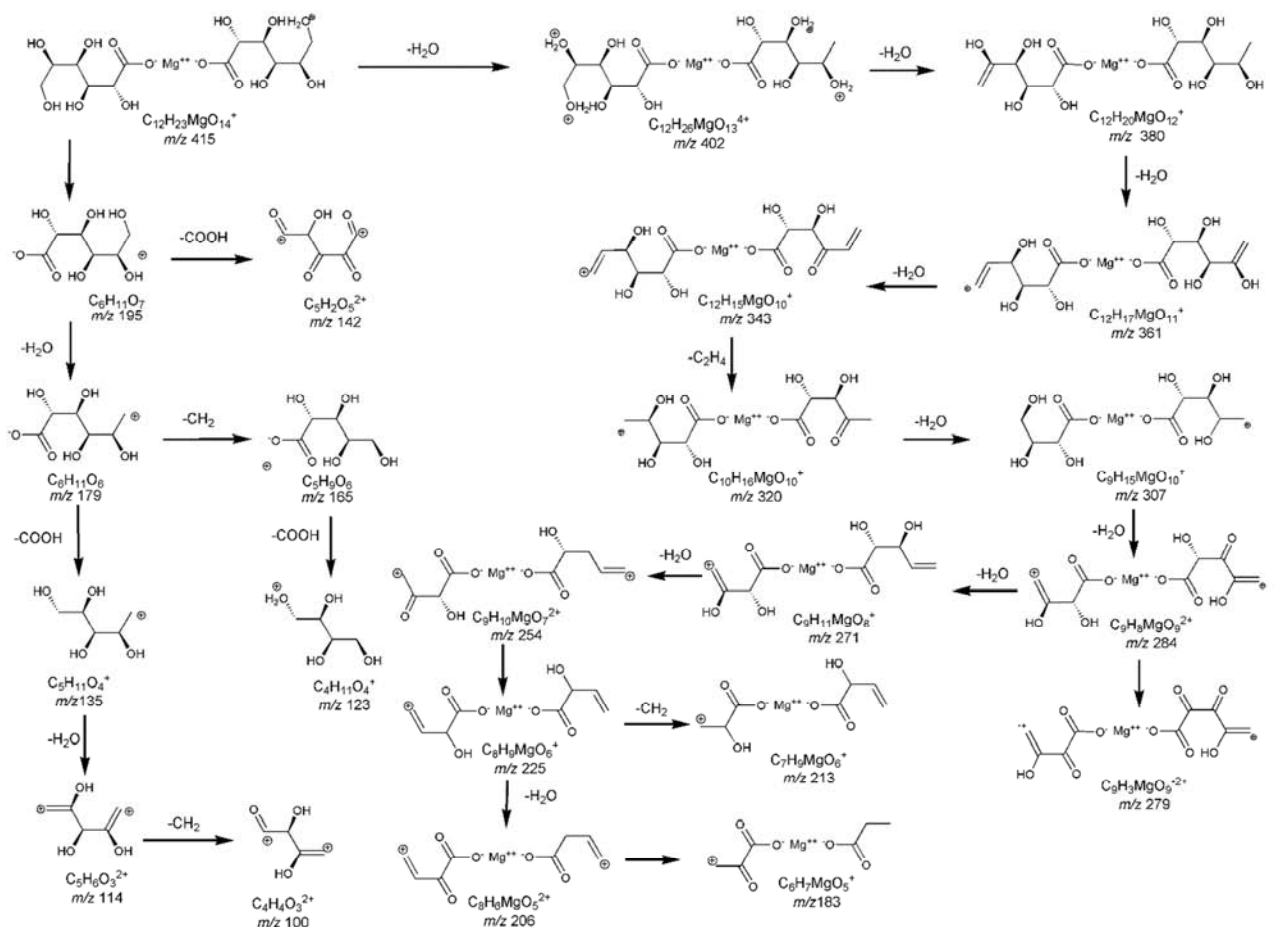


Figure 3. Proposed fragmentation pattern of magnesium gluconate.

The ESI-MS spectra of the control and treated samples (Figure 2) exhibited almost similar type fragmentation pattern. The fragment ion peak at  $m/z$  165 corresponding to  $C_5H_9O_6^+$  displayed 100% relative peak intensity in the ESI-MS spectrum of the control sample, while the highest intense peak was found in the ESI-MS spectrum of the treated sample at  $m/z$  114 corresponding to  $C_5H_6O_3^{2+}$  (Figure 2). The relative peak intensities of the other ion peaks in The Trivedi Effect<sup>®</sup> Treated sample were significantly changed compared with the control sample.

### 3.2. Isotopic Abundance Ratio Analysis

The molecular formula of magnesium gluconate is  $C_{12}H_{22}MgO_{14}$ . LC-MS spectra of both the control and treated samples indicated the presence of the mass for protonated molecular ion at  $m/z$  415 ( $C_{12}H_{23}MgO_{14}^+$ ) showing 28.56% and 26.84% relative intensity, respectively. The theoretical calculation of  $P_{M+1}$  and  $P_{M+2}$  for the protonated magnesium gluconate in the control sample was presented as below:

$$P(^{13}C) = [(12 \times 1.1\%) \times 28.56\% \text{ (the actual size of the } M^+ \text{ peak)}] / 100\% = 3.77\%$$

$$P(^2H) = [(23 \times 0.015\%) \times 28.56\%] / 100\% = 0.10\%$$

$$P(^{17}O) = [(14 \times 0.04\%) \times 28.56\%] / 100\% = 0.16\%$$

$$P(^{25}Mg) = [(1 \times 12.66\%) \times 28.56\%] / 100\% = 3.62\%$$

$$P_{M+1} \text{ i.e. } ^{13}C, ^2H, ^{17}O, \text{ and } ^{25}Mg \text{ contributions from } (C_{12}H_{23}MgO_{14})^+ \text{ to } m/z \text{ 416} = 7.65\%$$

From the above calculation, it has been found that  $^{13}C$  and  $^{25}Mg$  have major contribution to  $m/z$  416.

In the similar way,  $P_{M+2}$  can be calculated as follow:

$$P(^{18}O) = [(14 \times 0.20\%) \times 28.56\%] / 100\% = 0.80\%$$

$$P(^{26}Mg) = [(1 \times 13.94\%) \times 28.56\%] / 100\% = 3.98\%$$

So,  $P_{M+2}$  i.e.  $^{18}O$  and  $^{26}Mg$  contributions from

$$(C_{12}H_{23}MgO_{14})^+ \text{ to } m/z \text{ 417} = 4.78\%.$$

The above calculation indicated that  $^{13}C$  and  $^{25}Mg$  have the major contributions from magnesium gluconate to the isotopic peaks.

$P_M$  = the relative peak intensity of the parent molecular ion [ $M^+$ ];  $P_{M+1}$  = the relative peak intensity of the isotopic molecular ion [ $(M+1)^+$ ],  $P_{M+2}$  = the relative peak intensity of the isotopic molecular ion [ $(M+2)^+$ ], and  $M$  = mass of the parent molecule.

LC-MS spectra of the control and treated samples indicated the presence of the mass for the protonated magnesium gluconate ( $m/z$  415). Hence,  $P_M$ ,  $P_{M+1}$ , and  $P_{M+2}$  for magnesium gluconate at  $m/z$  415, 416, and 417 of the control and treated samples were obtained from the observed relative peak intensities of [ $M^+$ ], [ $(M+1)^+$ ], and [ $(M+2)^+$ ] peaks, respectively in the respective ESI-MS spectra are

presented in Table 2. The isotopic abundance ratio of  $P_{M+1}/P_M$  in the treated sample was significantly decreased by 48.87% compared to the control sample (Table 2). Consequently, the percentage change in the isotopic abundance ratio of  $P_{M+2}/P_M$  was significantly increased by 29.18% in the Biofield Energy Treated sample compared with the control sample. Thus,  $^{13}C$ ,  $^2H$ ,  $^{17}O$ , and  $^{25}Mg$  contributions from  $(C_{12}H_{23}MgO_{14})^+$  to  $m/z$  416;  $^{18}O$  and  $^{26}Mg$  contributions from  $(C_{12}H_{23}MgO_{14})^+$  to  $m/z$  417 in The Trivedi Effect<sup>®</sup> Treated sample were significantly changed compared to the control sample.

**Table 2.** Isotopic abundance analysis results of the magnesium gluconate ion in the control and Biofield Energy Treated sample.

Parameter	Control sample	Biofield Energy Treated sample
$P_M$ at $m/z$ 415 (%)	28.56	26.84
$P_{M+1}$ at $m/z$ 416 (%)	10.84	5.21
$P_{M+1}/P_M$	0.3796	0.1941
% Change of isotopic abundance ratio ( $P_{M+1}/P_M$ ) with respect to the control sample		-48.87
$P_{M+2}$ at $m/z$ 417 (%)	7.75	9.41
$P_{M+2}/P_M$	0.2714	0.3506
% Change of isotopic abundance ratio ( $P_{M+2}/P_M$ ) with respect to the control sample		29.18

Scientific literature [37-39, 45] reported that the vibrational energy is closely related with the reduced mass ( $\mu$ ) of the compound and the alteration of the vibrational energy can affect the several properties like physicochemical, thermal properties of the molecule. The relation between the vibrational energy and the reduced mass ( $\mu$ ) for a diatomic molecule is expressed as below [42, 45]:

$$E_o = \frac{h}{4\pi} \sqrt{\frac{f}{\mu}} \quad (2)$$

Where,  $E_o$  = the vibrational energy of a harmonic oscillator at absolute zero or zero point energy

$$f = \text{force constant}$$

$$\mu = \text{reduced mass} = \frac{m_a m_b}{m_a + m_b} \quad (3)$$

Where,  $m_a$  and  $m_b$  are the masses of the constituent atoms.

**Table 3.** Possible isotopic bond and their effect in the vibrational energy in magnesium gluconate molecule.

S. No.	Probable isotopic bond	Isotope type	Reduced mass ( $\mu$ )	Zero point vibrational energy ( $E_o$ )
1	$^{12}C-^{12}C$	Lighter	6.00	Higher
2	$^{13}C-^{12}C$	Heavier	6.26	Smaller
3	$^1H-^{12}C$	Lighter	0.92	Higher
4	$^2H-^{12}C$	Heavier	1.04	Smaller
5	$^{12}C-^{16}O$	Lighter	6.86	Higher
6	$^{13}C-^{16}O$	Heavier	7.17	Smaller
7	$^{12}C-^{17}O$	Heavier	7.03	Smaller
8	$^{12}C-^{18}O$	Heavier	7.20	Smaller
9	$^{16}O-^1H$	Lighter	0.94	Higher

S. No.	Probable isotopic bond	Isotope type	Reduced mass ( $\mu$ )	Zero point vibrational energy ( $E_0$ )
10	$^{16}\text{O}-^2\text{H}$	Heavier	1.78	Smaller
11	$^{24}\text{Mg}-^{16}\text{O}$	Lighter	9.60	Higher
12	$^{25}\text{Mg}-^{16}\text{O}$	Heavier	9.76	Smaller
13	$^{26}\text{Mg}-^{16}\text{O}$	Heavier	9.91	Smaller
14	$^{24}\text{Mg}-^{17}\text{O}$	Heavier	9.95	Smaller
15	$^{24}\text{Mg}-^{18}\text{O}$	Heavier	10.29	Smaller

The alteration in the isotopic abundance ratios of  $^{13}\text{C}/^{12}\text{C}$  for C-O;  $^2\text{H}/^1\text{H}$  for C-H and O-H bonds;  $^{17}\text{O}/^{16}\text{O}$  and  $^{18}\text{O}/^{16}\text{O}$  for C-O bond;  $^{25}\text{Mg}/^{24}\text{Mg}$ ,  $^{26}\text{Mg}/^{24}\text{Mg}$ ,  $^{17}\text{O}/^{16}\text{O}$  and  $^{18}\text{O}/^{16}\text{O}$  for Mg-O bond have the significant impact on the ground state vibrational energy of the molecule due to the higher reduced mass ( $\mu$ ) as shown in the Table 3 that leads to the isotope effects of the molecule.

Mass spectroscopic analysis of the several organic compounds revealed that the isotopic abundance of  $[\text{M}+1]^+$  and  $[\text{M}+2]^+$  ions were increased or decreased, thereby suggesting the change in number of neutrons in the molecule. It was then postulated to the alterations in atomic mass and atomic charge through possible mediation of neutrino oscillation [37-39, 46]. Thus, it is assumed that The Trivedi Effect<sup>®</sup> - Energy of

Consciousness Healing Treatment might offer the required energy for the neutrino oscillations. The changes of neutrinos inside the molecule in turn modified the particle size, chemical reactivity, density, thermal behavior, selectivity, binding energy, etc. [46]. The variation in the isotopic abundance ratio of one of the atoms in the reactants in a chemical reaction produces kinetic isotope effect. This effect is very useful to study the enzyme mechanism and also for understanding the enzymatic transition state that is helpful for designing enormously effective and specific inhibitors [42, 45, 47]. As magnesium is a vital cofactor for various enzymatic reactions, The Trivedi Effect<sup>®</sup> Treated magnesium gluconate that had altered isotopic abundance ratio might be beneficial for the study of enzyme mechanism as well as support in the designing of novel potent enzyme inhibitors.

### 3.3. Nuclear Magnetic Resonance (NMR) Analysis

The  $^1\text{H}$  and  $^{13}\text{C}$  NMR spectra of the control and treated magnesium gluconate are presented in the Figures 4 and 5, respectively.

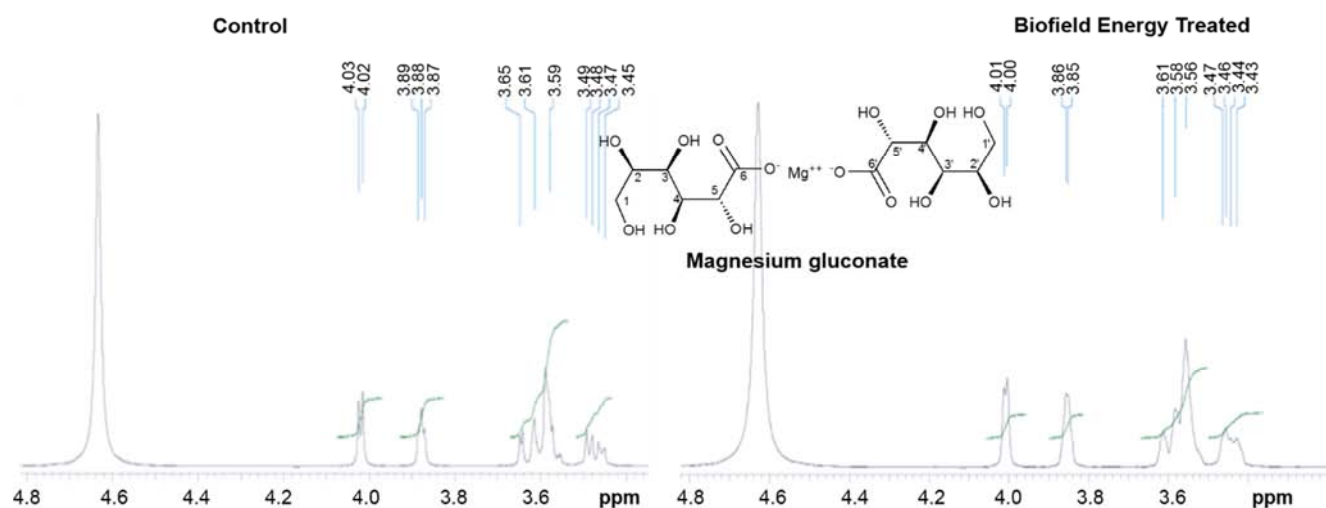


Figure 4. The  $^1\text{H}$  NMR spectra of the control and Biofield Energy Treated magnesium gluconate.

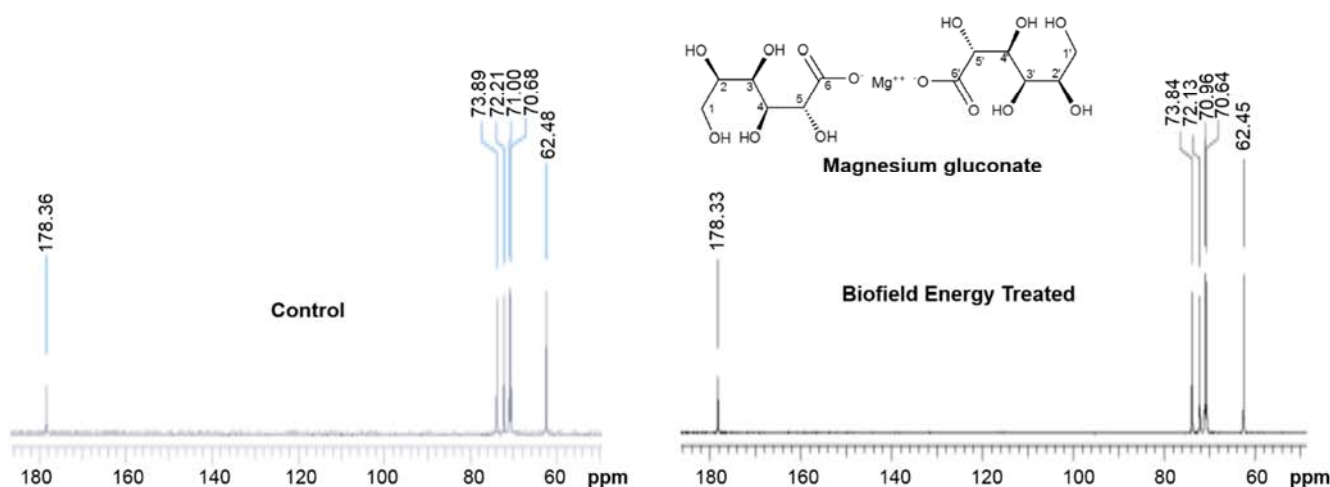


Figure 5. The  $^{13}\text{C}$  NMR spectra of the control and Biofield Energy Treated magnesium gluconate.

**Table 4.**  $^1\text{H}$  NMR and  $^{13}\text{C}$  NMR spectroscopic data of both the control and Biofield Energy Treated of magnesium gluconate.

Position	$^1\text{H}$ NMR $\delta$ (ppm)			$^{13}\text{C}$ NMR $\delta$ (ppm)	
	Number	Control	Treated	Control	Treated
1, 1'	4H <sup>*</sup>	3.65 (br s), 3.47 ( dd, $J = 12, 4$ Hz )	3.61 (br s), 3.45 ( dd, $J = 12, 4$ Hz )	62.48	62.45
2, 2'	2H <sup>*</sup>	3.59 (br s)	3.56 (br s)	70.68	70.64
3, 3'	2H <sup>*</sup>	3.61 (br s)	3.58 (br s)	71.00	70.96
4, 4'	2H	3.88 (br s)	3.86 (br s)	72.21	72.13
5, 5'	2H	4.03 (d, $J = 4$ Hz)	4.01 (d, $J = 4$ Hz)	73.89	73.84
6, 6'	--	--	--	178.36	178.33

br- broad, s- singlet, d- doublet, and dd- doublet of doublet, \* These assignments can be switched.

NMR assignments of the control and Biofield Energy Treated magnesium gluconate are shown in the Table 4. Although magnesium gluconate contains a large number of hydroxyl (OH) groups, the proton spectra of both the control and treated samples did not show any signal for the hydroxyl protons due to the replacement of the hydroxyl protons by deuterium from deuterated water, which was used as solvent for spectra recording. The signals for the protons coupling of  $\text{CH}_2$  group and adjacent CH protons (2-5) in the gluconic acid portion were observed in the control in the range of  $\delta$  3.47 to 4.03 ppm, these signals were found in the treated samples in the range of  $\delta$  3.45 to 4.01 ppm (Table 4), which was almost in accordance with the proton spectrum of sodium gluconate [48]. Similarly, the carbon signals for CO group,  $\text{CH}_2$  and CH groups in the  $^{13}\text{C}$  NMR spectrum of the treated sample were almost similar compared with the control sample (Table 4). So, the structure of the magnesium gluconate in the treated sample remained identical with the control sample.

## 4. Conclusions

The present study results demonstrated the structural characterization of magnesium gluconate using LC-MS and NMR techniques with a significant impact of The Trivedi Effect<sup>®</sup> - Energy of Consciousness Healing Treatment on the isotopic abundance ratios of  $\text{P}_{\text{M}+1}/\text{P}_{\text{M}}$  and  $\text{P}_{\text{M}+2}/\text{P}_{\text{M}}$ . The LC-MS analysis of the both control and treated samples showed the presence of the mass of the protonated magnesium gluconate at  $m/z$  415 at the retention time of 1.52 min with almost same type of fragmentation. Subsequently, the relative peak intensities of the fragment ions of The Trivedi Effect<sup>®</sup> Treated sample were significantly changed compared to the control sample. The isotopic abundance ratio of  $\text{P}_{\text{M}+1}/\text{P}_{\text{M}}$  ( $^2\text{H}/^1\text{H}$  or  $^{13}\text{C}/^{12}\text{C}$  or  $^{17}\text{O}/^{16}\text{O}$  or  $^{25}\text{Mg}/^{24}\text{Mg}$ ) was significantly decreased in the Biofield Energy Treated sample by 48.87% compared with the control sample. Consequently, the percentage change in the isotopic abundance ratio of  $\text{P}_{\text{M}+2}/\text{P}_{\text{M}}$  ( $^{18}\text{O}/^{16}\text{O}$  or  $^{26}\text{Mg}/^{24}\text{Mg}$ ) was significantly increased by 29.18% in the treated sample compared to the control sample. Briefly,  $^{13}\text{C}$ ,  $^2\text{H}$ ,  $^{17}\text{O}$ , and  $^{25}\text{Mg}$  contributions from  $(\text{C}_{12}\text{H}_{23}\text{MgO}_{14})^+$  to  $m/z$  416;  $^{18}\text{O}$  and  $^{26}\text{Mg}$  contributions from  $(\text{C}_{12}\text{H}_{23}\text{MgO}_{14})^+$  to  $m/z$  417 in the treated sample were significantly altered compared with the control sample. The treated sample might display isotope effects such as different physicochemical and thermal

properties, rate of the reaction, selectivity and binding energy due to its altered isotopic abundance ratios of  $\text{P}_{\text{M}+1}/\text{P}_{\text{M}}$  and  $\text{P}_{\text{M}+2}/\text{P}_{\text{M}}$  compared to the control sample. The Trivedi Effect<sup>®</sup> Treated magnesium gluconate might be supportive to understand the enzymatic reactions as well as to design the novel potent enzyme inhibitors using its kinetic isotope effects. Besides, The Trivedi Effect<sup>®</sup> - Energy of Consciousness Healing Treatment could be a useful approach for the design of better nutraceutical and/or pharmaceutical formulations that can provide significant therapeutic responses against various diseases such as diabetes mellitus, allergies and septic shock, stress-related disorders like sleep disorder, insomnia, anxiety, depression, Attention Deficit Disorder (ADD), Attention Deficit Hyperactive Disorder (ADHD), mental restlessness (mind chattering), brain fog, low libido, impotency, lack of motivation, mood swings, fear of the future, confusion, migraines, headaches, forgetfulness, overwhelm, loneliness, worthlessness, indecisiveness, frustration, irritability, chronic fatigue, obsessive/compulsive behavior and panic attacks, inflammatory diseases and immunological disorders like Lupus, Systemic Lupus Erythematosus, Hashimoto Thyroiditis, Type 1 Diabetes, Asthma, Chronic peptic ulcers, Tuberculosis, Hepatitis, Chronic active hepatitis, Celiac Disease (gluten-sensitive enteropathy), Addison Disease, Crohn's disease, Graves' Disease, Pernicious and Aplastic Anemia, Sjogren Syndrome, Irritable Bowel Syndrome (IBS), Multiple Sclerosis, Rheumatoid arthritis, Chronic periodontitis, Ulcerative colitis, Chronic sinusitis, Myasthenia Gravis, Atherosclerosis, Vasculitis, Dermatitis, Diverticulitis, Rheumatoid Arthritis, Reactive Arthritis, Alopecia Areata, Psoriasis, Scleroderma, Fibromyalgia, Chronic Fatigue Syndrome and Vitiligo, aging-related diseases like cardiovascular disease, arthritis, cancer, Alzheimer's disease, dementia, cataracts, osteoporosis, diabetes, hypertension, glaucoma, hearing loss, Parkinson's Disease, Huntington's Disease, Prion Disease, Motor Neurone Disease, Spinocerebellar Ataxia, Spinal muscular atrophy, Amyotrophic lateral sclerosis, Friedreich's Ataxia and Lewy Body Disease, chronic infections and many more.

## Abbreviations

A: Element; LC-MS: Liquid chromatography-mass spectrometry; M: Mass of the parent molecule;  $m/z$ : Mass-to-charge ratio; n: Number of the element; NMR: Nuclear



magnetic resonance spectroscopy;  $P_M$ : The relative peak intensity of the parent molecular ion  $[M^+]$ ;  $P_{M+1}$ : The relative peak intensity of isotopic molecular ion  $[(M+1)^+]$ ;  $P_{M+2}$ : The relative peak intensity of isotopic molecular ion  $[(M+2)^+]$ ;  $R_t$ : Retention time.

## Acknowledgements

The authors are grateful to GVK Biosciences Pvt. Ltd., Trivedi Science, Trivedi Global, Inc. and Trivedi Master Wellness for their assistance and support during this work.

## References

- [1] Ramachandran S, Fontanille P, Pandey A, Larroche C (2006) Gluconic acid: Properties, applications and microbial production. *Food Technol Biotechnol* 44: 185-195.
- [2] Heaton FW (1990) Role of magnesium in enzyme systems in metal ions in biological systems, In: Sigel H, Sigel A (Eds.), Volume 26: Compendium on magnesium and its role in biology, nutrition and physiology, Marcel Dekker Inc., New York.
- [3] Garfinkel L, Garfinkel D (1985) Magnesium regulation of the glycolytic pathway and the enzymes involved. *Magnesium* 4:60-72.
- [4] Swaminathan R (2003) Magnesium metabolism and its disorders. *Clin Biochem Rev* 24:47-66.
- [5] Gröber U, Schmidt J, Kisters K (2015) Magnesium in prevention and therapy. *Nutrients* 7:8199-8226.
- [6] William JH, Danziger J (2016) Magnesium deficiency and proton-pump inhibitor use: A clinical review. *J Clin Pharmacol* 56:660-668.
- [7] Guerrero MP, Volpe SL, Mao JJ (2009) Therapeutic uses of magnesium. *Am Fam Physician* 80:157-162.
- [8] Coudray C, Rambeau M, Feillet-Coudray C, Gueux E, Tressol JC, Mazur A, Rayssiguier Y (2005) Study of magnesium bioavailability from ten organic and inorganic Mg salts in Mg-depleted rats using a stable isotope approach. *Magn Res* 18:215-223.
- [9] Fleming TE, Mansmann Jr HC (1999) Methods and compositions for the prevention and treatment of diabetes mellitus. United States Patent 5871769, 1-10.
- [10] Fleming TE, Mansmann Jr HC (1999) Methods and compositions for the prevention and treatment of immunological disorders, inflammatory diseases and infections. United States Patent 5939394, 1-11.
- [11] Weglicki WB (2000) Intravenous magnesium gluconate for treatment of conditions caused by excessive oxidative stress due to free radical distribution. United States Patent 6100297, 1-6.
- [12] Turner RJ, Dasilva KW, O'Connor C, van den Heuvel C, Vink R (2004) Magnesium gluconate offers no more protection than magnesium sulphate following diffuse traumatic brain injury in rats. *J Am Coll Nutr* 23: 541S-544S.
- [13] Martin RW, Martin JN Jr, Pryor JA, Gaddy DK, Wiser WL, Morrison JC (1988) Comparison of oral ritodrine and magnesium gluconate for ambulatory tocolysis. *Am J Obstet Gynecol* 158:1440-1445.
- [14] Lee KH, Chung SH, Song JH, Yoon JS, Lee J, Jung MJ, Kim JH (2013) Cosmetic compositions for skin-tightening and method of skin-tightening using the same. United States Patent 8580741 B2.
- [15] Stenger VJ (1999) Bioenergetic fields. *Sci Rev Alternative Med* 3.
- [16] Sances F, Flora E, Patil S, Spence A, Shinde V (2013) Impact of biofield treatment on ginseng and organic blueberry yield. *Agrivita* 35:22-29.
- [17] Hammerschlag R, Jain S, Baldwin AL, Gronowicz G, Lutgendor SK, Oschman JL, Yount GL (2012) Biofield research: A roundtable discussion of scientific and methodological issues. *J Altern Complement Med* 18: 1081-1086.
- [18] Rubik B (2002) The biofield hypothesis: Its biophysical basis and role in medicine. *J Altern Complement Med* 8:703-717.
- [19] Koithan M (2009) Introducing complementary and alternative therapies. *J Nurse Pract* 5:18-20.
- [20] Trivedi MK, Branton A, Trivedi D, Nayak G, Mondal SC, Jana S (2015) Morphological characterization, quality, yield and DNA fingerprinting of biofield energy treated alphonso mango (*Mangifera indica* L.). *Journal of Food and Nutrition Sciences* 3:245-250.
- [21] Trivedi MK, Branton A, Trivedi D, Nayak G, Gangwar M, Jana S (2015) Agronomic characteristics, growth analysis, and yield response of biofield treated mustard, cowpea, horse gram, and groundnuts. *International Journal of Genetics and Genomics* 3:74-80.
- [22] Trivedi MK, Branton A, Trivedi D, Nayak G, Mondal SC, Jana S (2015) Effect of biofield treated energized water on the growth and health status in chicken (*Gallus gallus domesticus*). *Poult Fish Wildl Sci* 3:140.
- [23] Trivedi MK, Branton A, Trivedi D, Nayak G, Mondal SC, Jana S (2015) Antibiofilm of biofield-treated *Shigella boydii*: Global burden of infections. *Science Journal of Clinical Medicine* 4:121-126.
- [24] Trivedi MK, Patil S, Shettigar H, Gangwar M, Jana S (2015) An effect of biofield treatment on multidrug-resistant *Burkholderia cepacia*: A multihost pathogen. *J Trop Dis* 3:167.
- [25] Trivedi MK, Patil S, Shettigar H, Mondal SC, Jana S (2015) The potential impact of biofield treatment on human brain tumor cells: A time-lapse video microscopy. *J Integr Oncol* 4:141.
- [26] Trivedi MK, Branton A, Trivedi D, Nayak G, Mishra RK, Jana S (2015) Physicochemical evaluation of biofield treated peptone and malmgren modified terrestrial orchid medium. *American Journal of Bioscience and Bioengineering* 3:169-177.
- [27] Trivedi MK, Branton A, Trivedi D, Nayak G, Singh R, Jana S (2015) Physicochemical characterization of biofield treated orchid maintenance/replate medium. *Journal of Plant Sciences* 3:285-293.

- [28] Trivedi MK, Nayak G, Tallapragada RM, Patil S, Latiyal O, Jana S (2015) Effect of biofield treatment on structural and morphological properties of silicon carbide. *J Powder Metall Min* 4:132.
- [29] Trivedi MK, Tallapragada RM, Branton A, Trivedi D, Nayak G, Latiyal O, Jana S (2015) Evaluation of atomic, physical and thermal properties of tellurium powder: Impact of biofield energy treatment. *J Electr Electron Syst* 4:162.
- [30] Trivedi MK, Patil S, Shettigar H, Bairwa K, Jana S (2015) Spectroscopic characterization of chloramphenicol and tetracycline: An impact of biofield. *Pharm Anal Acta* 6:395.
- [31] Trivedi MK, Patil S, Shettigar H, Bairwa K, Jana S (2015) Spectroscopic characterization of biofield treated metronidazole and tinidazole. *Med chem* 5:340-344.
- [32] Trivedi MK, Tallapragada RM, Branton A, Trivedi D, Nayak G, Latiyal O, Jana S (2015) Potential impact of biofield treatment on atomic and physical characteristics of magnesium. *Vitam Miner* 3:129.
- [33] Trivedi MK, Tallapragada RM, Branton A, Trivedi D, Nayak G, Mishra RK, Jana S (2015) Biofield treatment: A potential strategy for modification of physical and thermal properties of gluten hydrolysate and ipomoea macroelements. *J Nutr Food Sci* 5:414.
- [34] Trivedi MK, Tallapragada RM, Branton A, Trivedi D, Nayak G, Mishra RK, Jana S (2015) Characterization of physical, spectroscopic and thermal properties of biofield treated biphenyl. *American Journal of Chemical Engineering*. 3:58-65.
- [35] Trivedi MK, Tallapragada RM, Branton A, Trivedi D, Nayak G, Mishra RK, Jana S (2015) Characterization of physical and thermal properties of biofield treated neopentyl glycol. *Pharm Anal Chem Open Access* 6:101.
- [36] MK, Branton A, Trivedi D, Nayak G, Saikia G, Jana S (2015) Mass Spectrometry Analysis of isotopic abundance of  $^{13}\text{C}$ ,  $^2\text{H}$ , or  $^{15}\text{N}$  in biofield energy treated aminopyridine derivatives. *American Journal of Physical Chemistry* 4:65-70.
- [37] Trivedi MK, Branton A, Trivedi D, Nayak G, Saikia G, Jana S (2015) Quantitative determination of isotopic abundance ratio of  $^{13}\text{C}$ ,  $^2\text{H}$ , and  $^{18}\text{O}$  in biofield energy treated ortho and meta toluic acid isomers. *American Journal of Applied Chemistry* 3:217-223.
- [38] Trivedi MK, Branton A, Trivedi D, Nayak G, Sethi KK, Jana S (2016) Isotopic abundance ratio analysis of biofield energy treated indole using gas chromatography-mass spectrometry. *Science Journal of Chemistry* 4:41-48.
- [39] Trivedi MK, Branton A, Trivedi D, Nayak G, Panda P, Jana S (2016) Evaluation of the isotopic abundance ratio in biofield energy treated resorcinol using gas chromatography-mass spectrometry technique. *Pharm Anal Acta* 7:481.
- [40] Schellekens RC, Stellaard F, Woerdenbag HJ, Frijlink HW, Kosterink JG (2011) Applications of stable isotopes in clinical pharmacology. *Br J Clin Pharmacol* 72:879-897.
- [41] Muccio Z, Jackson GP (2009) Isotope ratio mass spectrometry. *Analyst* 134: 13-222.
- [42] Vanhaecke F, Kyser K (2012) Isotopic composition of the elements In *Isotopic Analysis: Fundamentals and applications using ICP-MS* (1stedn), Edited by Vanhaecke F, Degryse P. Wiley-VCH GmbH & Co. KGaA, Weinheim.
- [43] Smith RM (2004) *Understanding Mass Spectra: A Basic Approach*, Second Edition, John Wiley & Sons, Inc, ISBN 0-471-42949-X.
- [44] Meija J, Coplen TB, Berglund M, Brand WA, De Bièvre P, Groning M, Holden NE, Irrgeher J, Loss RD, Walczyk T, Prohaska T (2016) Isotopic compositions of the elements 2013 (IUPAC technical Report). *Pure Appl Chem* 88:293-306.
- [45] Asperger S (2003) *Chemical Kinetics and Inorganic Reaction Mechanisms* Springer science + Business media, New York.
- [46] Trivedi MK, Mohan TRR (2016) Biofield energy signals, energy transmission and neutrinos. *American Journal of Modern Physics* 5:172-176.
- [47] Cleland WW (2003) The use of isotope effects to determine enzyme mechanisms. *J Biol Chem* 278:51975-51984.
- [48] Nikolic VD, Illic DP, Nikolic LB, Stanojevic LP, Cakic MD, Tacic AD, Ilic-Stojanovic SS (2014) The synthesis and characterization of iron (II) gluconate. *Advanced technologies* 3:16-24.